

Indirect optical manipulation of the antiferromagnetic order of insulating NiO by ultrafast interfacial energy transfer

Stephan Wust,^{1,*} Christopher Seibel,¹ Hendrik Meer,² Paul Herrgen,¹ Christin Schmitt,² Lorenzo Baldrati,² Rafael Ramos,^{3,4} Takashi Kikkawa,⁵ Eiji Saitoh,^{5,6,4,7} Olena Gomonay,² Jairo Sinova,^{2,8} Yuriy Mokrousov,^{2,9} Hans Christian Schneider,¹ Mathias Kläui,² Baerbel Rethfeld,¹ Benjamin Stadtmüller,^{1,2,†} and Martin Aeschlimann¹

¹*Department of Physics and Research Center OPTIMAS,*

Technische Universität Kaiserslautern, 67663 Kaiserslautern, Germany

²*Institute of Physics, Johannes Gutenberg-University Mainz, 55099 Mainz, Germany*

³*CIQUS, Departamento de Química-Física, Universidade de Santiago de Compostela, Santiago de Compostela, Spain*

⁴*WPI Advanced Institute for Materials Research, Tohoku University, Sendai 980-8577, Japan*

⁵*Department of Applied Physics, The University of Tokyo, Tokyo 113-8656, Japan*

⁶*Institute for AI and Beyond, The University of Tokyo, Tokyo 113-8656, Japan*

⁷*Advanced Science Research Center, Japan Atomic Energy Agency, Tokai 319-1195, Japan*

⁸*Institute of Physics, Czech Academy of Sciences,*

Cukrovarnická 10, 162 00 Praha 6, Czech Republic

⁹*Peter Grünberg Institut and Institute for Advanced Simulation,*

Forschungszentrum Jülich and JARA, 52425 Jülich, Germany.

(Dated: May 6, 2022)

We report the ultrafast, (sub)picosecond reduction of the antiferromagnetic order of the insulating NiO thin film in a Pt/NiO bilayer. This reduction of the antiferromagnetic order is not present in pure NiO thin films after a strong optical excitation. This ultrafast phenomenon is attributed to an ultrafast and highly efficient energy transfer from the optically excited electron system of the Pt layer into the NiO spin system. We propose that this energy transfer is mediated by a stochastic exchange scattering of hot Pt electrons at the Pt/NiO interface.

The recent discovery of current-driven torques in anti-ferromagnets (AFMs) has opened a pathway for the realization of a novel class of spintronic devices with attractive features compared to ferromagnetic spintronic devices. The zero net magnetization in the ground state of AFMs and the absence of magnetic stray fields allow for extremely high bit packing densities of the AFM-based functional units [1, 2]. In addition, the high-frequency magnon modes in the THz regime can potentially result in higher writing speeds in AFMs that can surpass the typical GHz operation speeds of ferromagnetic (FM) spintronic devices [3, 4].

In this regard, one of the most crucial challenges in anti-ferromagnetic spintronics is to optimize the speed and efficiency of the manipulation of the antiferromagnetic order that is characterized by the Néel vector. While current-driven manipulation of the Néel order by spin-orbit torques is a highly promising and reliable approach for storing information in AFMs [3, 5, 6], its operation speed is still limited to the timescale of current pulses, which is typically in the order of several tens to hundreds of picoseconds [2, 7]. Faster manipulation of the Néel order can be achieved by optical excitation of the AFM spin system. Pioneering studies have demonstrated the collective excitation of the spin system by THz and near-infrared (near-IR) excitation [3, 8–10]. Due to the electrically insulating nature of many AFMs, the spin system is directly excited by the electromagnetic light field via resonant excitation by the magnetic field component of the radiation [11], inelastic impulsive stimulated Raman

scattering [12], or d-d excitations [13, 14]. All these excitations result in coherent precessions of the Néel vector with frequencies of up to a few THz corresponding to a response of the spin-system on the picosecond timescale [10, 15].

An even faster response of the spin system of AFMs can potentially be achieved by strong non-equilibrium excitation of the material using fs-light pulses. This approach has already been demonstrated extensively for ferromagnetic materials for which an optical excitation with near-IR fs light pulses results in an incoherent loss of the magnetic order within a few hundreds of femtoseconds [16–22]. This so-called ultrafast demagnetization is however predominantly observed for metallic (ferromagnetic) systems for which the optical excitation results in a strong non-equilibrium excitation of the material’s electron system, which subsequently transfers its energy to the spin system [23, 24]. This excitation scheme is, however, not possible for a wide range of AFMs, which are largely insulators with bandgaps of several eV.

In our work, we demonstrate an alternative approach to incoherently manipulate the spin order of insulating antiferromagnet nickel oxide (NiO) on (sub-)picosecond timescale using fs near-IR pulses with photon energies below the bandgap of the insulating material. This is achieved by an ultrafast energy transfer from an adjacent metallic platinum (Pt) layer that is strongly excited by the ultrashort near-IR pulse. We propose that this ultrafast energy transfer occurs directly between the hot electron system of the metallic layer and the spin system

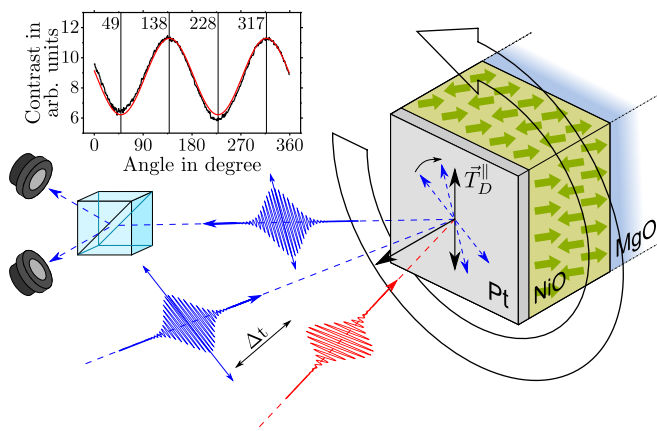


FIG. 1: Schematic illustration of the experimental approach to record the magnetic response of NiO by its magneto-optical birefringence (MOBF) signal. Changing the azimuthal orientation between the polarization of the probe beam and the projected in-plane anisotropy axis \vec{T}_D^{\parallel} of the AFM NiO results in a significant change in the rotation of the light polarization as shown in the inset. The response of the MOBF signal after a time Δt after the optical excitation is monitored in a pump-probe experiment. See supporting material for more details on the experiment.

of the insulating antiferromagnet and is mediated by a stochastic exchange scattering at the interface.

As the insulating AFM, we consider the model system NiO. NiO is a collinear wide bandgap AFM ($E_{\text{gap}} = 4.3 \text{ eV}$ [25]) and a promising candidate for possible spintronic applications due to its high Néel temperature of $T_N = 523 \text{ K}$ in the bulk [26], the possibility to electrically read and manipulate the antiferromagnetic order [27–29], and the observations of ultrafast currents in the THz regime in Pt/NiO bilayers structures [11, 30]. Below T_N , NiO is an easy plane antiferromagnet with a ferromagnetic exchange coupling of the spins within the $\{111\}$ planes and an antiferromagnetic coupling between spins of adjacent $\{111\}$ planes. Due to the NiO crystal symmetry, this results in the formation of four differently oriented twin-domains (T-domains), each consisting of three spin-domains (S-domains). In a bulk crystal, this leads to the coexistence of 12 antiferromagnetic domains [26, 31, 32].

In our study, we focus on a 10 nm thin NiO thin film capped with a 2 nm Pt layer grown on a MgO(001) substrate [33]. In this case, the additional strain from the substrate leads to a preferential out-of-plane orientation of the Néel vector of NiO [34, 35]. This reduces the number of S-domains for each T-domain and in essence, leads to a single S-domain state within each T-domain [29].

The ultrafast response of the spin system of NiO is monitored experimentally by the change in the magneto-optical birefringence (MOBF) signal in an all-optical pump-probe setup as shown in Fig. 1. The MOBF of NiO is the result of a rhombohedral distortion of the NiO

crystal lattice in its AFM phase which was observed both for bulk crystals [36] as well as for NiO thin films [33, 37]. This rhombohedral distortion associated with the magnetic AFM order leads to an anisotropy axis along the direction of the T-Domain \vec{T}_D^{\parallel} ($\langle 111 \rangle$) and thus to a different reflectivity of light with parallel and perpendicular polarization with respect to this anisotropy axis. This difference in reflectivity of the light field components can be detected as a rotation of light polarization of linearly polarized laser light after the reflection from the sample. We monitor the change in the orientation of the linearly polarized probe laser beam (photon energy 3.1 eV) in our experiment by using a polarization-sensitive balancing detector [37], see Fig. 1. In normal incidence geometry, we can continuously rotate the azimuthal orientation of the light polarization within the surface plane, which results in a sinusoidal oscillation of the detected signal (further explained in supplementary material). The periodicity of 180° of the signal matches the symmetry of the rhombohedral distortion of the NiO crystal lattice. This clearly demonstrates that our normal incidence experiment is sensitive enough to detect the magneto-optical birefringence signal despite the fact that we are only able to access the projection of the anisotropy axis in the plane of the sample surface \vec{T}_D^{\parallel} .

In our pump-probe experiment, we use an almost collinear normal incidence geometry of the linearly polarized pump and probe beam. The photon energy of the pump beam is 1.55 eV and hence significantly smaller than the optical band gap of NiO. We recorded time-resolved MOBF traces for two orientations of 45° and -45° of the probe beam polarization with respect to the anisotropy axis. Subtracting these traces with antisymmetric MOBF contributions (see inset Fig. 1) from each other allows us to eliminate pure optical signals that are expected to be symmetric in both traces.

We start the discussion of our experimental findings with the ultrafast magnetic response of a bare NiO(001) thin film as well as of the Pt/NiO(001) bilayer system after optical excitation in the near-IR range ($\hbar\omega = 1.55 \text{ eV}$). The time-resolved MOBF traces for both materials systems are shown in Figs. 2(a) and (b). We find no change in the transient MOBF signal for the bare NiO thin film. This is not surprising when considering NiO's large bandgap of 4.3 eV, which would require a three-photon absorption process to optically excite the NiO electron system. Such a process is, however, extremely unlikely for the absorbed laser fluences used in our experiment [38].

This situation changes drastically for the Pt(2nm)/NiO bilayer structure as shown in Fig. 2(b). The MOBF signal reduces significantly on a fs timescale followed by a slow relaxation of the signal on a timescale of several tens of picoseconds. The reduction of the MOBF signal is attributed to a reduction of the antiferromagnetic order in NiO. This conclusion is based on a

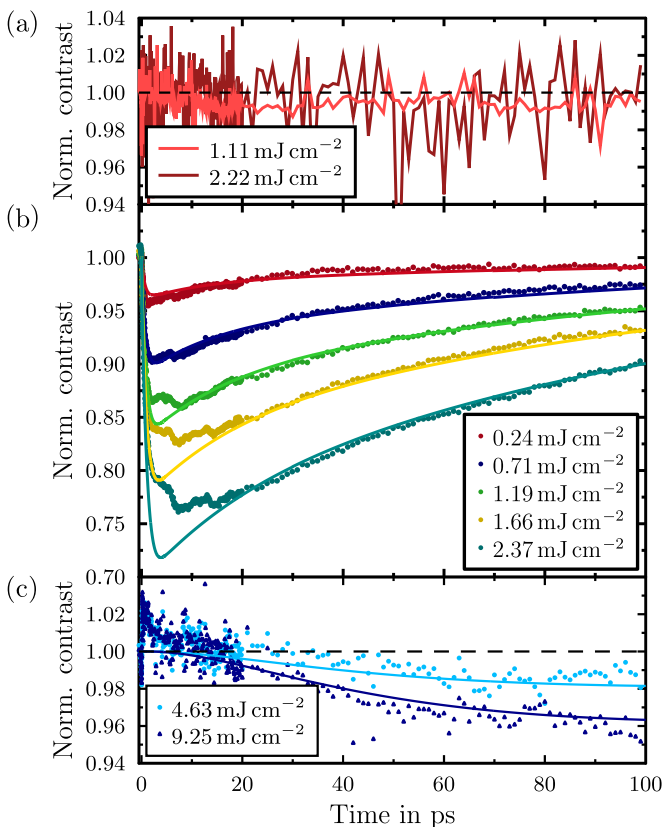


FIG. 2: Temporal evolution of the MOBF signal for three different samples after the optical excitation with 1.55 eV pump photons, and normal incidence geometry: (a) pure NiO. (b) a Pt(2 nm)/NiO bilayer structure, and (c) a Pt(2 nm)/MgO(3 nm)/NiO multilayer structure. (a) only represents experimental data. For (b) and (c) the experimental data are shown as colored dots, while the solid lines represent simulated MOBF traces that were obtained by a temperature-based model simulation.

recent time-resolved diffraction study which revealed a clear correlation between the reduction of the rhombohedral distortion of NiO and the change in the AFM order of the system [39]. Moreover, the transient MOBF traces reveal a coherent oscillation with a frequency of 130 GHz that is superimposed onto the incoherent MOBF signal [8–10]. The oscillation is most clearly visible for large fluences (see supporting materials). The frequency of this oscillation can be attributed to the low-frequency magnon mode and hence to a coherent oscillation of the NiO spin system.

Overall, our experimental data clearly demonstrate an optically induced loss of the antiferromagnetic order for the Pt/NiO bilayer system after excitation in the near-IR range that is absent for the bare NiO film for comparable fluences. In addition, the almost linear correlation between the applied fluence and the reduction of the magnetic order parameter indicates that the ultrafast loss of antiferromagnetic order is due to a linear absorption of

light in the material stack. All these experimental observations point to light absorption in the metallic Pt layer and a subsequent ultrafast energy transfer from the Pt into the NiO layer.

To further examine the microscopic origin of the indirect excitation of the NiO spin system via the Pt layer, we repeated the same experiment for a similar structure with an additional 3 nm thick MgO buffer layer between Pt and the NiO layers. The introduction of an insulating interlayer suppresses any interaction between the electron system of Pt and the electron or spin system of NiO, respectively [40]. The experimental MOBF traces for the Pt/MgO/NiO multilayer structure are shown in Fig. 2(c). They only reveal a marginal reduction of the MOBF signal even for considerably larger absorbed fluences in Pt that evolves on the timescale of several tens of ps. This rather slow and inefficient coupling between the Pt and NiO layer via MgO can only be explained by a phonon-mediated energy transfer. Hence, this reference experiment also points to an efficient coupling between the Pt electron systems with the NiO spin system in the Pt/NiO bilayer structure.

This hypothesis is supported by temperature-based phenomenological simulations which allow us to gain insights into the energy transfer processes within the magnet bilayer system. Figure 3(a) illustrates the different degrees of freedom considered in our model as well as their coupling parameters. Similar to the conventional two-temperature model (TTM) [24], we describe the dynamics of the metallic Pt layer by electrons coupled to phonons via an electron-phonon coupling parameter g_{ep} [24]. The heat capacity of the electrons is dynamically calculated from a realistic density of states (DOS) obtained from density functional theory (DFT) [41]. The heat capacity of the phonon system is kept constant according to the Dulong-Petit law.

For the insulating AFM NiO, we can neglect the electron system due to the small photon energy of the optical excitation compared to the bandgap. However, we treat the spin system as a separate subsystem as it is frequently done when modeling magnetization dynamics on ultrafast timescales [16, 23]. The heat capacity of the spin system is obtained from the measured total heat capacity [42], subtracting the phononic contribution. It exhibits a sharp peak at the Néel temperature due to the antiferromagnetic/paramagnetic phase transition [43]. The coupling between the spin system and the phonons is mediated by the magneto-elastic (spin-phonon) coupling g_{sp} [44, 45].

The most important parameters in our simulation describe the coupling mechanisms across the Pt/NiO interface. The large bandgap of NiO prevents particle (charge carrier) transport across the interface. In contrast, energy can be exchanged between both layers by several processes. The laser-heated electron system of Pt can couple directly to the phonons of the insulating NiO [46–

49]. However, this coupling was found to be important only on the ps to ns timescales [49] and is therefore not considered in our model. Instead, the main interaction channel involves a direct interaction of the Pt electrons with the NiO spins described by the electron-spin coupling parameter σ_{es} . Experimental evidence for the existence of such a direct coupling was recently found in a Pt/YIG bilayer structure [50]. Its physical origin can be interpreted as a torque induced in the spin system of the insulating layer by statistic scattering of metal electrons at the interface between both materials. A further energy dissipation channel is introduced to the MgO substrate. It is mediated by a phonon-phonon coupling mechanism, which is, however, too ineffective to contribute to the energy transfer across the Pt/NiO interface [49].

The energy or heat transfer between the Pt and NiO subsystems is calculated by solving the differential equations of the coupled layer-TTMs numerically [51]. The full set of equations is discussed in the supporting material. The energy or heat is distributed homogeneously within the different subsystems of the materials and we do not explicitly consider any depth-dependent variations within a single layer.

The optical excitation is modeled by a Gaussian laser pulse of varying fluence and a pulse duration of 50 fs (full width at half maximum) which excites the electron system of Pt. Figure 3(b) shows the results of our simulation for an exemplary laser fluence, and a set of typical coupling parameters. It thus shows the time-dependent temperature changes of all subsystems after optical excitation. The optically excited Pt electron system transfers its energy quickly to the Pt phonon system as well as into the NiO spin system thereby increasing the temperatures of these two systems. This results in equilibration of these three sub-systems within the first 5 ps to almost the same quasi-equilibrium temperature [52]. Subsequently, all three subsystems reduce their temperature by dissipating energy into the still cold NiO phonon system.

To compare our simulations with the experimental findings, we translate the spin temperature into the experimental signal $\delta MOBF$. We assume a quasi-instantaneous correlation between the lattice distortion and the temperature-induced changes of the antiferromagnetic order parameter [39] and exploit the known temperature-dependence of the MOBF, which is given as

$$\delta MOBF \propto \langle M \rangle_T^2 \propto (T_N - T_S)^{2\beta} \quad (1)$$

[53], where M is the magnetization of the sublattices, T_S is the simulated temperature of the NiO spin system, $T_N = 523$ K is the Néel temperature of NiO [37], and $\beta = 0.367$ is a critical exponent [53]. We compare the resulting theoretical MOBF trace with the experimental curve. We choose the data obtained for a fluence of 1.19 mJ cm^{-2} to optimize our four coupling parameters

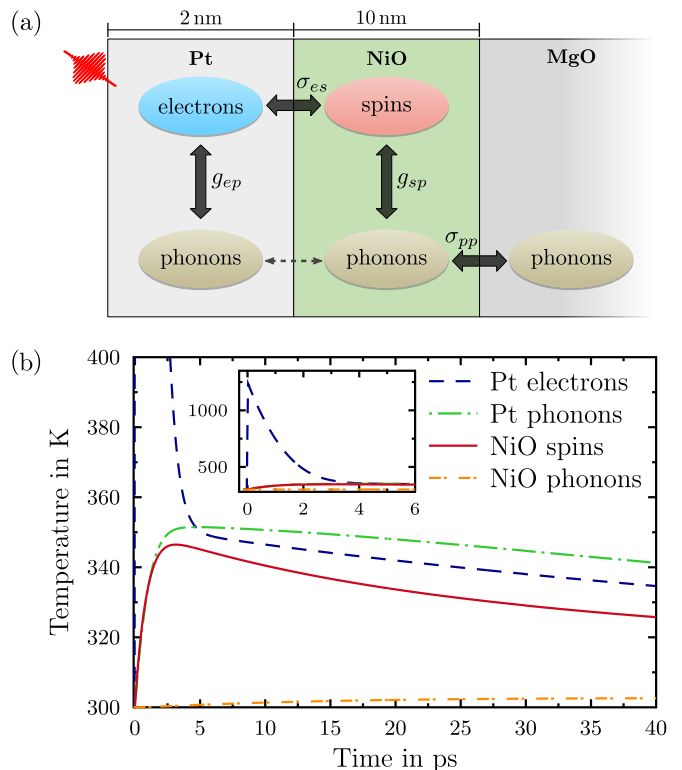


FIG. 3: (a) Illustration of the electron, spin and phonon subsystems of the different layers of the Pt/NiO bilayer system on a MgO substrate that are considered in our TTM simulations. The interaction channels are marked by thick black arrows between the subsystems. (b) Temporal evolution of the simulated temperatures in Pt and NiO. The temperature of the NiO spins determines the MOBF contrast.

g_{ep} , σ_{es} , g_{sp} and σ_{pp} , treated as independent on temperature. Here, g_{ep} and σ_{es} mainly drive the depth and time of the signal's minimum, respectively; g_{sp} the recovery-rate of the signal within tens of ps, and σ_{pp} the long-time behaviour towards the 100 ps-scale. Then, we calculate theoretical MOBF traces for the other fluences applied in the experiment.

The resulting curves show a very good fit with the experimental data, see Fig. 2 b). Our simulations reproduce the general trend observed in the experiment, i.e., we find a fast, (sub-) picosecond reduction of the magnetic signal followed by a significantly slower relaxation of the magnetic order. The MOBF dynamics observed for the Pt/NiO bilayer stack are very similar to the so-called demagnetization curves of metallic ferromagnetic materials after strong, non-equilibrium excitation in the near-IR range [16–22, 54]. However, in our case, the time constant of the loss of the antiferromagnetic order is between 0.5 and 1.0 ps and hence significantly longer than for a thin metallic ferromagnetic film, such as Ni or Co on an insulating substrate [16, 22]. The fast non-equilibrium dynamics of the MOBF signal can be attributed to the indirect heating through the optical

excitation of the adjacent non-magnetic metal layer. The characteristic timescale of this energy transfer is directly reflected in the temperature evolution of the NiO spin system shown in Fig. 3(b). It is heated by the Pt electrons within 500 fs to 1 ps. This ultrafast energy transfer is thus mediated by the direct coupling between the Pt electron and NiO spin system at the interface. This is further confirmed by introducing an insulating interlayer, as shown in Fig. 2(c). As discussed above, this suppresses this interfacial coupling and substantially reduces the speed and efficiency of the energy transfer from Pt into the NiO spin system; a situation that allows us to model the experimental data. In that case, excitation of the spin system of NiO proceeds solely through phonon-phonon coupling, which is considerably slower than the direct electron-spin coupling. We show the results of the corresponding simulation for the Pt/MgO/NiO multilayer system by a solid curve superimposed onto the experimental data in Fig. 2 c).

A discrepancy between the experimental and simulated MOBF traces, however, is the lineshape in the vicinity of the minimum of the magneto-optical contrast that is particularly visible for larger fluences in Fig. 2(b). As already discussed above, the systematically smaller reduction of the experimental MOBF signal can be explained by the coherent oscillation signal of the low-frequency magnon mode (130 GHz) [8–10] that is superimposed on the overall incoherent loss of the MOBF signal (see supporting material). In fact, a recent study shows that long-range collective spin-wave excitations of the magnetic system can be driven on the sub-ps scale by laser-excited hot electrons [55]. On this time scale, the laser-mediated coherent interaction between excited electrons and the spin subsystem can be understood as a result of non-equilibrium modifications to the exchange interactions which shake the spin system and ignite collective spin-wave excitations which *store* the excess energy invested into the electronic subsystem by the pulse, and survive over tens of picoseconds. Such contributions are, however, not explicitly included in our simplified model.

In conclusion, our joint experimental and theoretical study of the optically excited Pt/NiO bilayer system has uncovered an incoherent ultrafast loss of the antiferromagnetic order of NiO after optical excitation with fs pulses in the near-IR range, i.e., for photon energies below the NiO bandgap. The loss of the magnetic order occurs within the first ps after the optical excitation. Our experimental observation was attributed to an ultrafast energy transfer from the optically excited electron system in Pt directly into the antiferromagnetic spin system of NiO that depends on the coupling strength across the interface. We propose that this ultrafast energy transfer is mediated by an exchange coupling between excited electrons in Pt and the NiO spins at the interface. This coupling leads to an exchange of energy, but also of angular momentum between both layers. The missing spin

order in Pt causes a random exchange of angular momentum that results in an incoherent loss of magnetic order in NiO. In this way, our work lays the foundation for the ultrafast manipulation of the magnetic order of insulating and semiconducting (antiferromagnetic) materials by interface engineering and optical excitation below the optical bandgap.

The experimental work was funded by the Deutsche Forschungsgemeinschaft (DFG, German Research Foundation) - TRR 173 - 268565370 Spin + X: spin in its collective environment (Projects A01, A03, A08, A11, and B03). B.S. further acknowledges funding by the Dynamics and Topology Research Center (Top-Dyn) funded by the State of Rhineland Palatinate. R.R. acknowledges support from the European Commission through the project 734187-SPICOLST (H2020-MSCA-RISE-2016), the European Union’s Horizon 2020 research and innovation program through the MSCA grant agreement SPEC-894006, Grant RYC 2019-026915-I funded by the MCIN/AEI/ 10.13039/501100011033 and by ”ESF investing in your future”, the Xunta de Galicia (ED431B 2021/013, Centro Singular de Investigación de Galicia Accreditation 2019-2022, ED431G 2019/03) and the European Union (European Regional Development Fund - ERDF). Additionally, T.K. and E.S. acknowledge support from JST-CREST (JPMJCR20C1 and JPMJCR20T2), Grant-in-Aid for Scientific Research (JP19H05600 and JP20H02599) from JSPS KAKENHI, Japan, and Institute for AI and Beyond of the University of Tokyo.

* Electronic address: wust@rhrk.uni-kl.de

† Electronic address: bstadtmueller@physik.uni-kl.de

- [1] V. Baltz, A. Manchon, M. Tsoi, T. Moriyama, T. Ono, and Y. Tserkovnyak, *Rev. Mod. Phys.* **90**, 015005 (2018), URL <https://journals.aps.org/rmp/abstract/10.1103/RevModPhys.90.015005>.
- [2] T. Jungwirth, J. Sinova, A. Manchon, X. Marti, J. Wunderlich, and C. Felser, *Nat. Phys* **14**, 200 (2018), URL <https://www.nature.com/articles/s41567-018-0063-6>.
- [3] K. Olejnik, T. Seifert, Z. Kašpar, V. Novák, P. Wadley, R. P. Campion, M. Baumgartner, P. Gambardella, P. Němec, J. Wunderlich, et al., *Sci. Adv.* **4**, eaar3566 (2018), URL <https://www.science.org/doi/full/10.1126/sciadv.aar3566>.
- [4] T. Satoh, S.-J. Cho, R. Iida, T. Shimura, K. Kuroda, H. Ueda, Y. Ueda, B. Ivanov, F. Nori, and M. Fiebig, *Phys. Rev. Lett.* **105**, 077402 (2010), URL <https://journals.aps.org/prl/abstract/10.1103/PhysRevLett.105.077402>.
- [5] S. Y. Bodnar, L. Šmejkal, I. Turek, T. Jungwirth, O. Gomonay, J. Sinova, A. Sapozhnik, H.-J. Elmers, M. Kläui, and M. Jourdan, *Nat. Commun.* **9**, 1 (2018), URL <https://www.nature.com/articles/s41467-017-02780-x>.

- [6] H. Meer, F. Schreiber, C. Schmitt, R. Ramos, E. Saitoh, O. Gomonay, J. Sinova, L. Baldrati, and M. Kläui, *Nano Lett.* **21**, 114 (2020), URL <https://pubs.acs.org/doi/abs/10.1021/acs.nanolett.0c03367>.
- [7] J. Železný, P. Wadley, K. Olejník, A. Hoffmann, and H. Ohno, *Nat. Phys.* **14**, 220 (2018), URL <https://www.nature.com/articles/s41567-018-0062-7>.
- [8] H. Qiu, L. Zhou, C. Zhang, J. Wu, Y. Tian, S. Cheng, S. Mi, H. Zhao, Q. Zhang, D. Wu, et al., *Nat. Phys.* **17**, 388 (2021), URL <https://www.nature.com/articles/s41567-020-01061-7>.
- [9] C. Tzschaschel, K. Otani, R. Iida, T. Shimura, H. Ueda, S. Günther, M. Fiebig, and T. Satoh, *Phys. Rev. B* **95**, 174407 (2017), URL <https://journals.aps.org/prb/abstract/10.1103/PhysRevB.95.174407>.
- [10] D. Bossini, M. Pancaldi, L. Soumah, M. Basini, F. Mertens, M. Cinchetti, T. Satoh, O. Gomonay, and S. Bonetti, *Phys. Rev. Lett.* **127**, 077202 (2021), URL <https://journals.aps.org/prl/abstract/10.1103/PhysRevLett.127.077202>.
- [11] T. Kampfrath, A. Sell, G. Klatt, A. Pashkin, S. Mährlein, T. Dekorsy, M. Wolf, M. Fiebig, A. Leitenstorfer, and R. Huber, *Nat. Photonics* **5**, 31 (2011), URL <https://www.nature.com/articles/nphoton.2010.259>.
- [12] D. Bossini, S. Dal Conte, Y. Hashimoto, A. Secchi, R. V. Pisarev, T. Rasing, G. Cerullo, and A. V. Kimel, *Nat. Commun.* **7**, 1 (2016), URL <https://www.nature.com/articles/ncomms10645?origin=ppub>.
- [13] X. Wang, R. Y. Engel, I. Vaskivskiy, D. Turenne, V. Shokeen, A. Yaroslavtsev, O. Grånäs, R. Knut, J. O. Schunck, S. Dziarzhyski, et al., arXiv preprint arXiv:2201.03280 (2022), URL <https://arxiv.org/abs/2201.03280>.
- [14] K. Gilmeister, D. Golež, C.-T. Chiang, N. Bittner, Y. Pavlyukh, J. Berakdar, P. Werner, and W. Widdra, *Nat. Commun.* **11**, 1 (2020), URL <https://www.nature.com/articles/s41467-020-17925-8>.
- [15] T. Satoh, R. Iida, T. Higuchi, Y. Fujii, A. Koreeda, H. Ueda, T. Shimura, K. Kuroda, V. Butrim, and B. Ivanov, *Nat. Commun.* **8**, 1 (2017).
- [16] E. Beaurepaire, J.-C. Merle, A. Daunois, and J.-Y. Bigot, *Phys. Rev. Lett.* **76**, 4250 (1996), URL <https://journals.aps.org/prl/abstract/10.1103/PhysRevLett.76.4250>.
- [17] B. Koopmans, J. J. M. Ruigrok, F. D. Longa, and W. J. M. de Jonge, *Phys. Rev. Lett.* **95**, 267207 (2005), URL <https://link.aps.org/doi/10.1103/PhysRevLett.95.267207>.
- [18] R. Medapalli, I. Razdolski, M. Savoini, A. Khor-sand, A. Kirilyuk, A. Kimel, T. Rasing, A. Kalash-nikova, A. Tsukamoto, and A. Itoh, *Phys. Rev. B* **86**, 054442 (2012), URL <https://journals.aps.org/prb/abstract/10.1103/PhysRevB.86.054442>.
- [19] M. Battiato, K. Carva, and P. M. Oppeneer, *Phys. Rev. Lett.* **105**, 027203 (2010), URL <https://journals.aps.org/prl/abstract/10.1103/PhysRevLett.105.027203>.
- [20] W. You, P. Tengdin, C. Chen, X. Shi, D. Zusin, Y. Zhang, C. Gentry, A. Blonsky, M. Keller, P. M. Oppeneer, et al., *Phys. Rev. Lett.* **121**, 077204 (2018), URL <https://journals.aps.org/prl/abstract/10.1103/PhysRevLett.121.077204>.
- [21] G. P. Zhang and W. Hübner, *Phys. Rev. Lett.* **85**, 3025 (2000), URL <https://link.aps.org/doi/10.1103/PhysRevLett.85.3025>.
- [22] J.-Y. Bigot, M. Vomir, L. Andrade, and E. Beau-repaire, *J. Chem. Phys.* **318**, 137 (2005), URL <https://www.sciencedirect.com/science/article/pii/S030101040500248X>.
- [23] B. Koopmans, G. Malinowski, F. Dalla Longa, D. Steiauf, M. Fähnle, T. Roth, M. Cinchetti, and M. Aeschlimann, *Nat. Mater.* **9**, 259 (2010), URL <https://www.nature.com/articles/nmat2593>.
- [24] S. I. Anisimov, B. L. Kapeliovich, and T. L. Perel'man, *Sov. Phys. JETP* **39**, 375 (1974), URL <http://www.jetp.ac.ru/cgi-bin/e/index/e/39/2/p375?a=list>.
- [25] G. Sawatzky and J. Allen, *Phys. Rev. Lett.* **53**, 2339 (1984), URL <https://journals.aps.org/prl/abstract/10.1103/PhysRevLett.53.2339>.
- [26] W. L. Roth, *J. Appl. Phys.* **31**, 2000 (1960), URL <http://aip.scitation.org/doi/10.1063/1.1735486>.
- [27] G. R. Hoogeboom, A. Aqeel, T. Kuschel, T. T. M. Palstra, and B. J. van Wees, *Appl. Phys. Lett.* **111**, 052409 (2017), URL <http://dx.doi.org/10.1063/1.4997588> <http://aip.scitation.org/doi/10.1063/1.4997588>.
- [28] T. Moriyama, K. Oda, T. Ohkochi, M. Kimata, and T. Ono, *Sci. Rep.* **8**, 14167 (2018), URL <http://dx.doi.org/10.1038/s41598-018-32508-w> <http://www.nature.com/articles/s41598-018-32508-w>.
- [29] C. Schmitt, L. Baldrati, L. Sanchez-Tejerina, F. Schreiber, A. Ross, M. Filianina, S. Ding, F. Fuhrmann, R. Ramos, F. Maccherozzi, et al., *Phys. Rev. Appl.* **15**, 034047 (2021), URL <https://link.aps.org/doi/10.1103/PhysRevApplied.15.034047>.
- [30] T. Moriyama, K. Hayashi, K. Yamada, M. Shima, Y. Ohya, and T. Ono, *Phys. Rev. Mater.* **4**, 074402 (2020), URL <https://link.aps.org/doi/10.1103/PhysRevMaterials.4.074402>.
- [31] W. L. Roth and G. A. Slack, *J. Appl. Phys.* **31**, S352 (1960), URL <http://aip.scitation.org/doi/10.1063/1.1984744>.
- [32] G. A. Slack, *J. Appl. Phys.* **31**, 1571 (1960), URL <http://aip.scitation.org/doi/10.1063/1.1735895>.
- [33] F. Schreiber, L. Baldrati, C. Schmitt, R. Ramos, E. Saitoh, R. Lebrun, and M. Kläui, *Appl. Phys. Lett.* **117**, 082401 (2020), URL <https://aip.scitation.org/doi/full/10.1063/5.0011852>.
- [34] D. Alders, L. H. Tjeng, F. C. Voogt, T. Hibma, G. A. Sawatzky, C. T. Chen, J. Vogel, M. Sacchi, and S. Iacobucci, *Phys. Rev. B* **57**, 11623 (1998), URL <https://link.aps.org/doi/10.1103/PhysRevB.57.11623>.
- [35] S. Altieri, M. Finazzi, H. H. Hsieh, H. J. Lin, C. T. Chen, T. Hibma, S. Valeri, and G. A. Sawatzky, *Phys. Rev. Lett.* **91**, 137201 (2003), URL <https://link.aps.org/doi/10.1103/PhysRevLett.91.137201>.
- [36] K. Germann, K. Maier, and E. Strauß, *Solid State Commun.* **14**, 1309 (1974), URL <https://linkinghub.elsevier.com/retrieve/pii/0038109874906541>.
- [37] J. Xu, C. Zhou, M. Jia, D. Shi, C. Liu, H. Chen, G. Chen, G. Zhang, Y. Liang, J. Li, et al., *Phys. Rev. B* **100**, 134413 (2019), URL <https://link.aps.org/doi/10.1103/PhysRevB.100.134413>.
- [38] B. Sun, Y. Zhang, R. Zhang, H. Yu, G. Zhou, H. Zhang, and J. Wang, *Adv. Opt. Mater.* **5**, 1600937 (2017), URL <https://onlinelibrary.wiley.com/doi/full/10.1002/adom.201600937>.
- [39] Y. W. Windsor, D. Zahn, R. Kamrta, J. Feldl, H. Seiler, C.-T. Chiang, M. Ramsteiner, W. Widdra,

- R. Ernstorfer, and L. Rettig, *Phys. Rev. Lett.* **126**, 147202 (2021), URL <https://journals.aps.org/prl/abstract/10.1103/PhysRevLett.126.147202>.
- [40] L. Mihalceanu, S. Keller, J. Greser, D. Karfaridis, K. Simeonidis, G. Vourlias, T. Kehagias, A. Conca, B. Hillebrands, and E. T. Papaioannou, *Appl. Phys. Lett.* **110**, 252406 (2017), URL <https://aip.scitation.org/doi/full/10.1063/1.4989678>.
- [41] Z. Lin, L. V. Zhigilei, and V. Celli, *Phys. Rev. B* **77**, 075133 (2008), URL <https://journals.aps.org/prb/abstract/10.1103/PhysRevB.77.075133>.
- [42] J. Keem and J. Honig, Center for Information and Numerical Data, Cindas Report **52** (1978), URL <https://apps.dtic.mil/sti/citations/ADA128940>.
- [43] R. Radwanski and Z. Ropka, *Acta Phys. Pol.* **114**, 213 (2008), URL <http://przyrbwn.icm.edu.pl/APP/PDF/114/a114z132.pdf>.
- [44] S. Wall, D. Prabhakaran, A. Boothroyd, and A. Cavalleri, *Phys. Rev. Lett.* **103**, 097402 (2009), URL <https://journals.aps.org/prl/abstract/10.1103/PhysRevLett.103.097402>.
- [45] E. Aytan, B. Debnath, F. Kargar, Y. Barlas, M. M. Lacerda, J. X. Li, R. K. Lake, J. Shi, and A. A. Balandin, *Appl. Phys. Lett.* **111**, 252402 (2017), URL <http://aip.scitation.org/doi/10.1063/1.5009598>.
- [46] M. Huberman and A. Overhauser, *Phys. Rev. B* **50**, 2865 (1994), URL <https://journals.aps.org/prb/abstract/10.1103/PhysRevB.50.2865>.
- [47] P. E. Hopkins, J. L. Kassebaum, and P. M. Norris, *J. Appl. Phys.* **105**, 023710 (2009), URL <https://aip.scitation.org/doi/full/10.1063/1.3068476>.
- [48] K. Sokolowski-Tinten, R. Li, A. H. Reid, S. P. Weathersby, F. Quirin, T. Chase, R. Coffee, J. Corbett, A. Fry, N. Hartmann, et al., *New J. Phys.* **17**, 113047 (2015), URL <https://iopscience.iop.org/article/10.1088/1367-2630/17/11/113047/meta>.
- [49] J. Lombard, F. Detcheverry, and S. Merabia, *J. Phys. Condens. Matter* **27**, 015007 (2014), URL <https://iopscience.iop.org/article/10.1088/0953-8984/27/1/015007/meta>.
- [50] T. S. Seifert, S. Jaiswal, J. Barker, S. T. Weber, I. Rzdolski, J. Cramer, O. Gueckstock, S. F. Maehrlein, L. Nadvornik, S. Watanabe, et al., *Nat. Commun.* **9**, 1 (2018), URL <https://www.nature.com/articles/s41467-018-05135-2>.
- [51] J. Crank and P. Nicolson, *Math. Proc. Camb. Philos. Soc.* **43**, 50–67 (1947).
- [52] J. Pudell, A. Maznev, M. Herzog, M. Kronseder, C. Back, G. Malinowski, A. von Reppert, and M. Bargheer, *Nat. Commun.* **9**, 1 (2018), URL <https://www.nature.com/articles/s41467-018-05693-5>.
- [53] V. Saidl, P. Nĕmec, P. Wadley, V. Hills, R. Champion, V. Novák, K. Edmonds, F. Maccherozzi, S. Dhesi, B. Gallagher, et al., *Nat. Photonics* **11**, 91 (2017), URL <https://www.nature.com/articles/nphoton.2016.255>.
- [54] B. Mueller, A. Baral, S. Vollmar, M. Cinchetti, M. Aeschlimann, H. Schneider, and B. Rethfeld, *Phys. Rev. Lett.* **111**, 167204 (2013), URL <https://journals.aps.org/prl/abstract/10.1103/PhysRevLett.111.167204>.
- [55] S. Ghosh, F. Freimuth, O. Gomonay, S. Blügel, and Y. Mokrousov, *Commun. Phys.* **5**, 1 (2022), URL <https://www.nature.com/articles/s42005-022-00840-3>.

Indirect optical manipulation of the antiferromagnetic order of insulating NiO by ultrafast interfacial energy transfer

Stephan Wust,^{1,*} Christopher Seibel,¹ Hendrik Meer,² Paul Herrgen,¹ Christin Schmitt,² Lorenzo Baldrati,² Rafael Ramos,^{3,4} Takashi Kikkawa,⁵ Eiji Saitoh,^{5,6,4,7} Olena Gomony,² Jairo Sinova,^{2,8} Yuriy Mokrousov,^{2,9} Hans Christian Schneider,¹ Mathias Kläui,² Baerbel Rethfeld,¹ Benjamin Stadtmüller,^{1,2,†} and Martin Aeschlimann¹

¹*Department of Physics and Research Center OPTIMAS,*

Technische Universität Kaiserslautern, 67663 Kaiserslautern, Germany

²*Institute of Physics, Johannes Gutenberg-University Mainz, 55099 Mainz, Germany*

³*CIQUS, Departamento de Química-Física, Universidade de Santiago de Compostela, Santiago de Compostela, Spain*

⁴*WPI Advanced Institute for Materials Research, Tohoku University, Sendai 980-8577, Japan*

⁵*Department of Applied Physics, The University of Tokyo, Tokyo 113-8656, Japan*

⁶*Institute for AI and Beyond, The University of Tokyo, Tokyo 113-8656, Japan*

⁷*Advanced Science Research Center, Japan Atomic Energy Agency, Tokai 319-1195, Japan*

⁸*Institute of Physics, Czech Academy of Sciences,*

Cukrovarnická 10, 162 00 Praha 6, Czech Republic

⁹*Peter Grünberg Institut and Institute for Advanced Simulation,*

Forschungszentrum Jülich and JARA, 52425 Jülich, Germany.

(Dated: May 6, 2022)

MAGNETO-OPTICAL BIREFRINGENCE

The magnetic order of the antiferromagnet NiO is monitored by its magneto-optical birefringence (MOBF). Below its Néel-temperature, NiO exhibits a rhombohedral distortion, which shows a uniaxial anisotropy in reflectivity [1]. Depending on the relative angle of this anisotropy axis to the linear polarization of the incoming light, this causes a rotation of polarization upon reflection on the sample [2].

$$\theta_{pol} = \frac{r_{\parallel} - r_{\perp}}{r_{\parallel} + r_{\perp}} \sin 2\varphi \quad (S1)$$

In this equation, r_{\parallel} and r_{\perp} are the reflection coefficients parallel and perpendicular to the in-plane projection of the distortion \vec{T}_D^{\parallel} , φ is the relative angle between the polarization of the incoming light and \vec{T}_D^{\parallel} , and θ_{pol} represents the resulting rotation of the polarization of the reflected probe beam [2]. This anisotropy axis is identified by rotating the sample by 360°. A sketch explaining the measurement geometry and the corresponding calibration curve are shown in Figs. S1(a) and (b).

In our time-resolved (pump-probe) experiment, we record the birefringence signal for two sample angles with antisymmetric MOBF contribution. This allows us to obtain a pure MOBF signal without pure optical contribution by subtracting these two experimental signals from each other. This procedure is well established for time-resolved Kerr studies of ferromagnetic materials.

EXPERIMENTAL DETAILS

Our time-resolved experiments were performed with an all-optical pump-probe setup using an amplified Ti:Sapphire laser system (1.55 eV, 35 fs, 1 kHz, 7 mJ per pulse) to generate the pump and probe beams. We determined the temporal pulse length at the sample position to 40 ± 3 fs for the 1.55 eV pump pulse and 47 ± 5 fs for the 3.1 eV probe pulse by employing auto- and cross-correlation methods. The probe was created by second-harmonic generation of the fundamental laser radiation with a Beta-Barium-Borate (BBO) crystal. Both s-polarized pulses were focused on the sample under normal incidence (Angle relative to sample normal $< 1^\circ$). Both beams were adjusted to the rotational center of the sample, to ensure probing and pumping the same sample position independent of the sample angle φ . The laser spot sizes used in our experiment are shown in the following section.

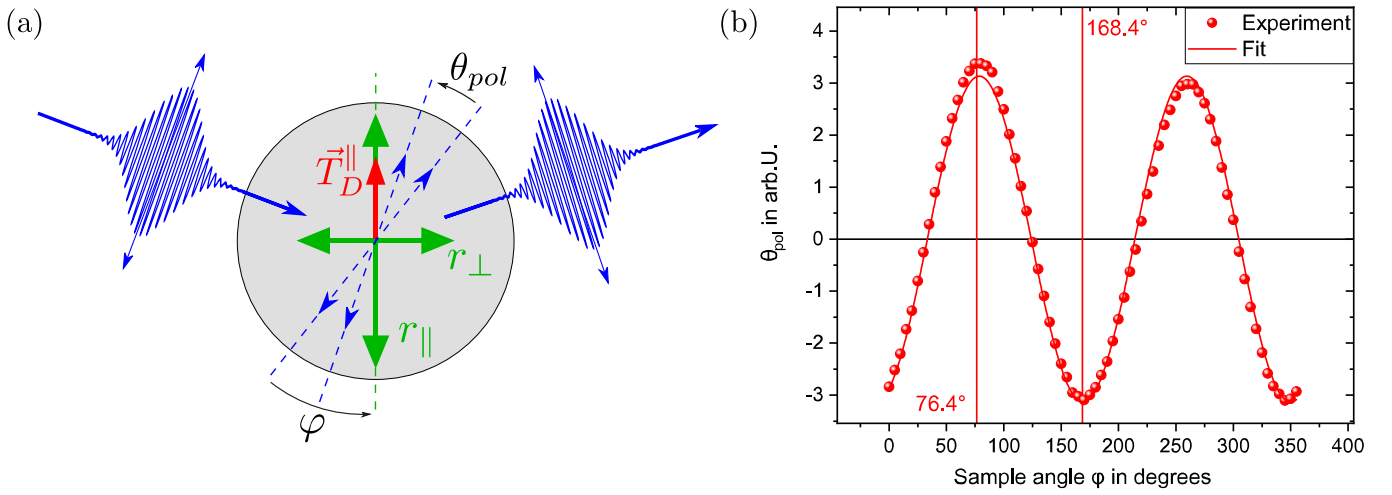


FIG. S1: (a) Detailed sketch explaining the measurement of the magneto-optical birefringence with an illustration of the variables shown in equation (S1). (b) Magneto-optical birefringence signal in dependency of the sample angle φ . Markings indicate the angles chosen for the time-resolved measurements.

DETERMINING THE APPLIED FLUENCE

For the applied pump fluences presented in the main manuscript, the spot size of the pump beam was determined with a CCD camera (see S2). The intensity profile of the resulting image was fitted by a two-dimensional Gaussian resulting in the $1/e^2$ -width of both beams. The size of the probe spot was chosen to be smaller than the pump spot.

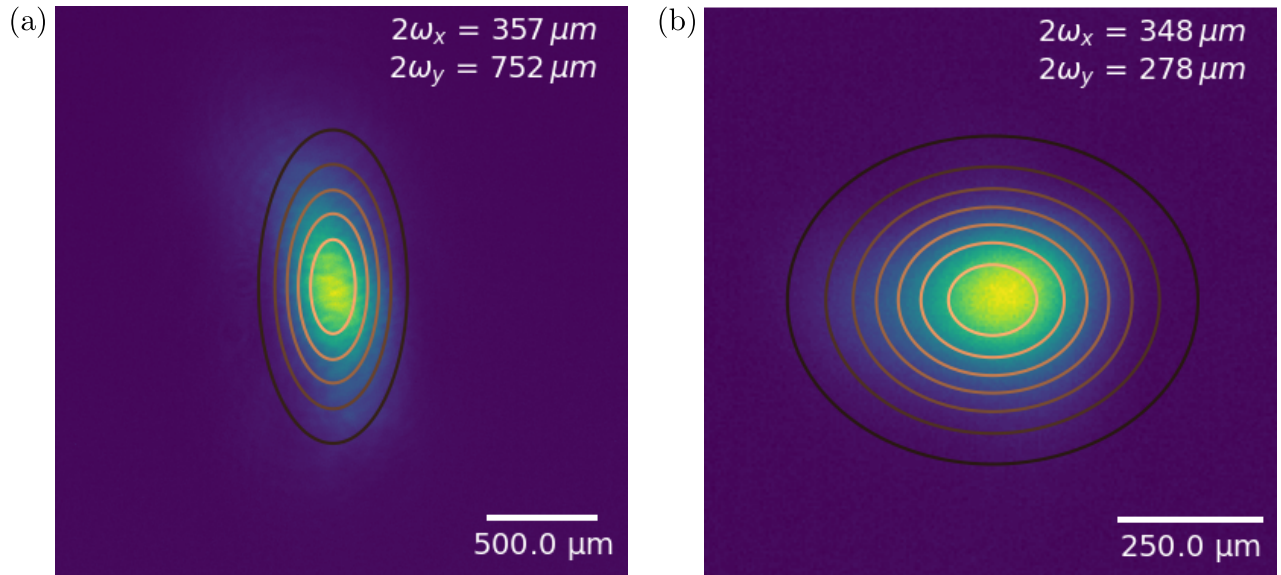


FIG. S2: Spot images of focused a) pump and b) probe beam. Images were fitted by a 2d-Gaussian function to determine the $1/e^2$ radii in x- and y-direction.

The total applied peak fluence was then determined using the following definition:

$$\Phi = \frac{2P}{f\pi w_x w_y} \quad (\text{S2})$$

Here P represents the applied laser power, f is the repetition rate of the laser while w_x and w_y are the corresponding $1/e^2$ spot-radii in x- and y-direction determined in Fig. S2 [3].

IDENTIFICATION OF MAGNON MODES

Here, we discuss the quantification of the frequency of the coherent magnon mode observed in our time-resolved MOBF experiment. In the first step, we subtracted a double exponential fit from the experimental data shown in Fig. 2(b) of the main manuscript. Afterward, a power spectrum (auto-correlated FFT) was applied to obtain the frequency spectrum in Figure S3.

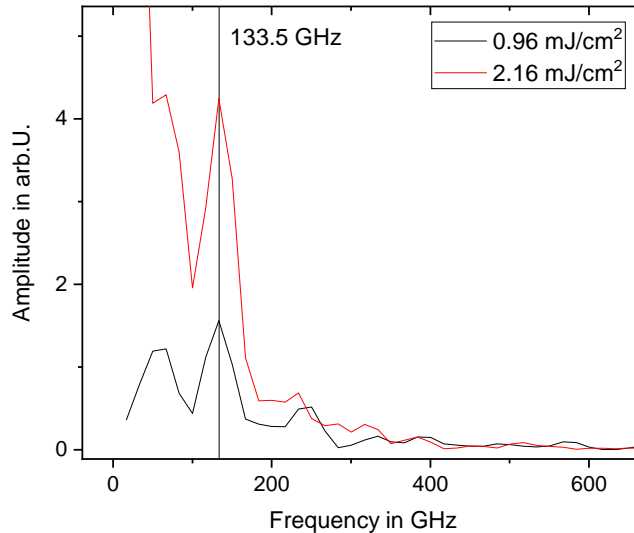


FIG. S3: Power spectrum of the time-resolved MOBF traces obtained for high fluences. The marked frequency of 133.5 GHz indicates the appearance of the low-frequency magnon mode in NiO.

The two extracted power spectra for the depicted fluences both show a clear peak around 133,5 GHz which very much resembles reported values for the low-frequency magnon mode in NiO [4–6]

MODEL-DESCRIPTION OF ENERGY FLOW

We describe the energy flow between the participating subsystems in the layers of the sample on the basis of a temperature-dependent phenomenological model. Due to the small thicknesses of the layers, the energy within the Pt layer as well as within the NiO layer is assumed to be distributed homogeneously. Therefore, transport effects within a layer can be neglected.

Similar to the two-temperature model (TTM) [7], we describe the dynamics of the metallic Pt layer by electrons coupled to phonons via an electron-phonon coupling parameter g_{ep} . Its magnitude is under continuous discussion; we start with a value of Medvedev and Milov [8]. The heat capacity of the electrons in Pt is dynamically calculated from a realistic density of states (DOS) obtained from density functional theory (DFT) [9], whereas for the phonons a constant heat capacity according to the Dulong-Petit law is used.

In the insulating antiferromagnet NiO, we apply the same expression for the phononic heat capacity as in Pt. However, there are no free electrons in the dielectric material. In the spirit of the model proposed by Beaurepaire et al. to explain their pioneering results [10], we consider the spins a separate system. The coupling between spins and phonons is mediated by magneto-elastic (spin-phonon) coupling g_{sp} [11, 12]. The heat capacity of the spin system is obtained by subtracting the phononic contribution from the measured total heat capacity [13]. It exhibits a sharp peak at the Néel temperature due to the antiferromagnetic/paramagnetic phase transition and does not contribute above the Neel temperature [14].

Possible coupling mechanisms across the Pt/NiO interface are electron-spin, electron-phonon and phonon-phonon coupling. The coupling mechanisms to the phonons act only on a pico- to nanosecond timescale [15] and are therefore disregarded in our model. The electron-spin coupling can be understood as in a Pt/YIG bilayer structure [16], where statistic scattering of metal electrons at the interface induce torques of the magnetic moments in the dielectric. We describe this interaction by an electron-spin coupling parameter σ_{es} .

We further introduce an energy sink at constant temperature T_0 which is mediated by the phonons of the MgO substrate, draining energy from the NiO phonons. The rate of the energy flow is determined by the thermal boundary conductance σ_{pp} , which can be obtained from the diffusive mismatch model (DMM) [17]. All energies transported across interfaces are homogeneously distributed across the respective materials of thicknesses d . Then, the model reads

$$c_{e,\text{Pt}} \frac{dT_{e,\text{Pt}}}{dt} = -g_{ep}(T_{e,\text{Pt}} - T_{p,\text{Pt}}) - \frac{\sigma_{es}}{d_{\text{Pt}}}(T_{e,\text{Pt}} - T_{s,\text{NiO}}) + s(t), \quad (\text{S3a})$$

$$c_{p,\text{Pt}} \frac{dT_{p,\text{Pt}}}{dt} = +g_{ep}(T_{e,\text{Pt}} - T_{p,\text{Pt}}), \quad (\text{S3b})$$

$$c_{s,\text{NiO}} \frac{dT_{s,\text{NiO}}}{dt} = -g_{sp}(T_{s,\text{NiO}} - T_{p,\text{NiO}}) + \frac{\sigma_{es}}{d_{\text{NiO}}}(T_{e,\text{Pt}} - T_{s,\text{NiO}}), \quad (\text{S3c})$$

$$c_{p,\text{NiO}} \frac{dT_{p,\text{NiO}}}{dt} = +g_{sp}(T_{s,\text{NiO}} - T_{p,\text{NiO}}) - \frac{\sigma_{pp}}{d_{\text{NiO}}}(T_{p,\text{NiO}} - T_0), \quad (\text{S3d})$$

where $s(t)$ is an energy source term accounting for the laser excitation. We apply the Crank-Nicolson scheme to solve the system of coupled differential equations (S3) numerically [18].

In our calculations, we use a Gaussian laser pulse of various fluences and 50 fs duration (FWHM) in agreement with our experiments. The four coupling parameters g_{ep} , σ_{es} , g_{sp} and σ_{pp} are taken as independent on temperature. While the energy loss of the laser-heated Pt electrons, described with the coupling parameters g_{ep} and σ_{es} , mainly influence the height and time of the peak of the spin temperature T_s , the coupling of the spin system to the phonons in NiO is responsible for the relaxation in the 10 ps range. The energy loss to the substrate, described by σ_{pp} , acts on a longer range of ~ 100 ps.

We optimize these four parameters in comparison with the experimental MOBF trace for an intermediate fluence of 1.19 mJ cm^{-2} . Excitation with other laser fluences is simulated with the same set of parameters.

* Electronic address: wust@rhrk.uni-kl.de

† Electronic address: bstadtmueller@physik.uni-kl.de

- [1] K. Germann, K. Maier, and E. Strauß, Solid State Commun. **14**, 1309 (1974), URL <https://linkinghub.elsevier.com/retrieve/pii/0038109874906541>.
- [2] J. Xu, C. Zhou, M. Jia, D. Shi, C. Liu, H. Chen, G. Chen, G. Zhang, Y. Liang, J. Li, et al., Phys. Rev. B **100**, 134413 (2019), URL <https://link.aps.org/doi/10.1103/PhysRevB.100.134413>.
- [3] R. Gort, K. Bühlmann, G. Saerens, S. Däster, A. Vaterlaus, and Y. Acremann, Applied Physics Letters **116**, 112404 (2020), URL <https://aip.scitation.org/doi/full/10.1063/1.5143115>.
- [4] C. Tzschaschel, K. Otani, R. Iida, T. Shimura, H. Ueda, S. Günther, M. Fiebig, and T. Satoh, Phys. Rev. B **95**, 174407 (2017), URL <https://journals.aps.org/prb/abstract/10.1103/PhysRevB.95.174407>.
- [5] T. Satoh, S.-J. Cho, R. Iida, T. Shimura, K. Kuroda, H. Ueda, Y. Ueda, B. Ivanov, F. Nori, and M. Fiebig, Phys. Rev. Lett. **105**, 077402 (2010), URL <https://journals.aps.org/prl/abstract/10.1103/PhysRevLett.105.077402>.
- [6] D. Bossini, M. Pancaldi, L. Soumah, M. Basini, F. Mertens, M. Cinchetti, T. Satoh, O. Gomonay, and S. Bonetti, Phys. Rev. Lett. **127**, 077202 (2021), URL <https://journals.aps.org/prl/abstract/10.1103/PhysRevLett.127.077202>.
- [7] S. I. Anisimov, B. L. Kapeliovich, and T. L. Perel'man, Sov. Phys. JETP **39**, 375 (1974), URL <http://www.jetp.ac.ru/cgi-bin/e/index/e/39/2/p375?a=list>.
- [8] N. Medvedev and I. Milov, Phys. Rev. B **102**, 064302 (2020), URL <https://link.aps.org/doi/10.1103/PhysRevB.102.064302>.
- [9] Z. Lin, L. V. Zhigilei, and V. Celli, Phys. Rev. B **77**, 075133 (2008), URL <https://journals.aps.org/prb/abstract/10.1103/PhysRevB.77.075133>.
- [10] E. Beaurepaire, J.-C. Merle, A. Daunois, and J.-Y. Bigot, Phys. Rev. Lett. **76**, 4250 (1996), URL <https://journals.aps.org/prl/abstract/10.1103/PhysRevLett.76.4250>.
- [11] S. Wall, D. Prabhakaran, A. Boothroyd, and A. Cavalleri, Phys. Rev. Lett. **103**, 097402 (2009), URL <https://journals.aps.org/prl/abstract/10.1103/PhysRevLett.103.097402>.
- [12] E. Aytan, B. Debnath, F. Kargar, Y. Barlas, M. M. Lacerda, J. X. Li, R. K. Lake, J. Shi, and A. A. Balandin, Appl. Phys. Lett. **111**, 252402 (2017), URL <http://aip.scitation.org/doi/10.1063/1.5009598>.

- [13] J. Keem and J. Honig, Center for Information and Numerical Data, Cindas Report **52** (1978), URL <https://apps.dtic.mil/sti/citations/ADA128940>.
- [14] R. Radwanski and Z. Ropka, Acta Phys. Pol. **114**, 213 (2008), URL <http://przyrbwn.icm.edu.pl/APP/PDF/114/a114z132.pdf>.
- [15] J. Lombard, F. Detcheverry, and S. Merabia, J. Phys. Condens. Matter **27**, 015007 (2014), URL <https://iopscience.iop.org/article/10.1088/0953-8984/27/1/015007/meta>.
- [16] T. S. Seifert, S. Jaiswal, J. Barker, S. T. Weber, I. Razdolski, J. Cramer, O. Gueckstock, S. F. Maehrlein, L. Nadvornik, S. Watanabe, et al., Nat. Commun. **9**, 1 (2018), URL <https://www.nature.com/articles/s41467-018-05135-2>.
- [17] E. Swartz and R. Pohl, Rev. Mod. Phys. **61**, 605 (1989), URL <https://journals.aps.org/rmp/abstract/10.1103/RevModPhys.61.605>.
- [18] J. Crank and P. Nicolson, Math. Proc. Camb. Philos. Soc. **43**, 50–67 (1947).